

jets observed at $E \geq 800$ Bev/nucleon. Carrying through a similar investigation we limited ourselves to α -particle jets having energies $E \geq 3000$ Bev/nucleon. In view of the discussion given above and in II we, however, think that the true lower limit of the energy is lowered by a factor of about 2 and hence is more like 1500 Bev/nucleon. From the 5 observed events, the geometry of our stack, and the exposure time of the stack we find a flux value of 3.6×10^{-3} α particles/m² sterad sec at $E \geq 1500$ Bev/nucleon. Assuming a detection efficiency of 100%, this yields a value of the exponent $\gamma = 1.58_{-0.18}^{+0.21}$. The limits of error include an uncertainty by a factor of 2, of both flux and energy. This

value of γ is in satisfactory agreement with the exponent derived for heavy nuclei of energies up to 100 Bev/nucleon and for α particles up to 7 Bev. There is no evidence for a substantial change in γ .

ACKNOWLEDGMENTS

We wish to thank Professor Marcel Schein for the possibility of carrying out this investigation and for his continuous interest and encouragement. We are greatly indebted to D. M. Haskin for his cooperation and to our scanning team for locating the events and for carrying out some of the calculations. We thank the Turin group for sending us some of their results prior to publication.

Intersecting-Beam Systems with Storage Rings

G. K. O'NEILL AND E. J. WOODS

Palmer Physical Laboratory, Princeton University, Princeton, New Jersey

(Received November 24, 1958)

The equivalence of fixed- and variable-field particle acceleration systems for the adiabatic damping of synchrotron oscillations is pointed out. These two quite different acceleration methods are therefore able to produce particle beams of equal density for beam stacking purposes.

The transfer mechanism between an accelerator and a storage ring is discussed, and the properties of a fast-rise 3-kilogauss beam-switching magnet are shown. It is concluded that the source interaction rate obtainable in a proton storage ring system would be nearly independent of the focusing properties and repetition rate of the injecting accelerator.

An improved design for intersecting-beam storage rings is described, in which several well-separated interaction regions could be used for simultaneous experiments. Standard types of alternating-gradient magnets would be required, and the over-all weight of synchrotron plus storage rings would be about one-tenth as large as that of comparable beam-stacking accelerators.

I. INTRODUCTION

INTERSECTING-BEAM devices have come to be recognized generally as a necessary next step in accelerator design, mainly as a result of the continuing efforts of the Midwestern Universities Research Association (MURA).¹ Within the last few years a number of designs for achieving high center-of-mass energies have been suggested.²⁻⁵ To obtain adequate interaction rates, it is necessary to accumulate ("stack") many pulses of accelerated particles near the maximum energy containable in the guide field. It has been shown that for proton accelerators one can only perform beam

stacking by filling the limited amount of available synchrotron and betatron oscillation phase space.⁶⁻⁸

There have been two approaches to intersecting-beam accelerator design. That of the MURA group has been through fixed-field alternating-gradient (FFAG) accelerators⁹ which are able to contain, within a single vacuum chamber, all energies from a few Mev up to the stacking energy. Although intersecting-beam FFAG synchrotrons would be large and would require complicated magnetic fields, they would accomplish their purpose within a single magnetic guide field region. Models have proven the design principles to be sound.

We have studied the alternative possibility of trans-

¹ Kerst, Cole, Crane, Jones, Laslett, Ohkawa, Sessler, Symon, Terwilliger, and Nilsen, *Phys. Rev.* **102**, 590 (1956).

² G. K. O'Neill, *Phys. Rev.* **102**, 1418 (1956).

³ G. K. O'Neill, *Proceedings of the CERN Symposium on High-Energy Accelerators and Pion Physics, Geneva, 1956* (European Organization of Nuclear Research, Geneva, 1956), p. 64.

⁴ T. Ohkawa, *Rev. Sci. Instr.* **29**, 108 (1958).

⁵ E. J. Woods and G. K. O'Neill, *Bull. Am. Phys. Soc. Ser. II*, **3**, 169 (1958); Princeton-Pennsylvania Accelerator Project, Internal Report GKO'N-11, December, 1957 (unpublished).

⁶ Symon, Stehle, and Lichtenberg, *Bull. Am. Phys. Soc. Ser. I*, **1**, 344 (1956).

⁷ G. K. O'Neill, *Bull. Am. Phys. Soc.* **1**, 344 (1956).

⁸ K. R. Symon and A. Sessler, *Proceedings of the CERN Symposium on High-Energy Accelerators and Pion Physics, Geneva, 1956* (European Organization of Nuclear Research, Geneva, 1956), p. 44.

⁹ Symon, Kerst, Jones, Laslett, and Terwilliger, *Phys. Rev.* **103**, 1837 (1956).

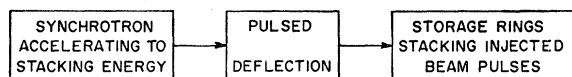


FIG. 1. Block diagram of storage ring stacking system.

ferring full-energy beam pulses from any accelerator (strong or weak focusing) into storage-ring guide fields made by simple magnet shapes, and stacking many full-energy pulses in the storage rings (see Fig. 1). This second approach depends critically on the development of a good ejector and injector. However, the ejection problem is simplified by the fact that the proton beam in a synchrotron is damped adiabatically to a small cross section as the magnetic field increases during the acceleration cycle. Betatron oscillations damp as $B^{-\frac{1}{2}}$ and synchrotron oscillations as B^{-1} .^{10,11} The full-energy beam can therefore be deflected by a pulsed magnet of small aperture.

In the following sections we will discuss the limitations which (despite apparent wide differences in design) are common to all intersecting-beam arrangements using particles other than electrons. We will then describe a beam storage system flexible enough to be adapted to most large accelerators, existing or planned. One new device—a pulsed magnet of fast rise time—is a necessary part of the system we describe; measurements made on a full-scale model of this magnet are given in Sec. IIIb.

II. CURRENT DENSITY LIMITS

Any intersecting-beam device so far suggested would make use of the following sequence of steps for operation: (a) injection of protons at an energy of 3 to 50 Mev from an electrostatic generator or linear accelerator; (b) capture into a focusing guide field; (c) acceleration by rf energy along a path of slowly increasing magnetic field; (d) stacking of many groups of particles in the guide field at high energy, forming a large circulating current. If acceleration takes place within a magnetic field fixed in time, it is possible (but not necessary) to include an additional step of stacking at an intermediate energy, and acceleration by various subharmonics of the rf frequency. If acceleration occurs in a time-varying guide field, each accelerated particle group must be transferred to a fixed guide field for stacking.

Any of three effects can set an upper limit to the circulating current attainable. These are (a) the long-range electromagnetic forces acting between charges moving in opposite directions (the interaction-region forces); (b) losses of particles from the stacked beam due to multiple scattering or nuclear interactions in the residual gas; and (c) the limited synchrotron and betatron oscillation phase space available at the stacking energy.

Given very good injection and acceleration systems, and high vacua, (a) will presumably remain an ultimate limit. This effect has been discussed,^{12,13} but not in published reports. Estimates made in these references show that effect (a), while certainly much more severe than the single-beam space-charge limit, is not so serious as to prevent the attainment of adequate beam-on-beam interaction rates.

Effect (b), and any others which reduce the lifetime of the stacked beams, determine the current of particles which must be delivered to the stacking energy. The acceleration system must supply a current Q/t to the stacking energy, with Q the design value of circulating charge and t the beam lifetime. In order to reduce background, any beam storage system will use an ultra-high vacuum (10^{-8} to 10^0 mm). Two laboratories are now building such vacuum systems for use on electron beam storage devices; their design is based on vacuum technology already developed in thermonuclear power research. At 10^{-8} mm, the mean life of a relativistic proton against large-angle single scattering or nuclear interaction is about 30 hours. The lifetime against multiple Coulomb scattering can be obtained by solving the Fokker-Planck equation for losses of protons to the vacuum chamber walls. At 3 Bev the lifetime against this loss is about equal to the nuclear interaction time.

Limit (c) depends on the intensity and the angular and energy spread of the low-energy injector, and on the adiabatic damping of betatron and synchrotron oscillations which takes place during the acceleration cycle. Given an injector of a particular energy and design, the only differences in principle among various acceleration schemes are in repetition rate and in the damping they produce. It seems reasonable that the damping factors should depend only on the ratio of initial to final magnetic fields. This can be shown to be true, but the fact has been unintentionally concealed by wide differences in notation in the literature. For time-varying fields, Twiss and Frank (reference 11) noted that the amplitudes of radial and vertical betatron oscillations damp as $B^{-\frac{1}{2}}$, at all energies. They obtained the damping of energy (synchrotron) oscillations by direct solution of the equations of motion, and independently by finding a generalized momentum p_ψ associated with the azimuthal angle ψ . Translating their Eqs. (22) into coordinates ψ and $x=r-r_0$, with r_0 the central equilibrium orbit, their result is that area in (x,ψ) space damps as B^{-1} . In addition, their Eq. (18) describes independently the damping of x and ψ under adiabatic field changes.

The damping of betatron oscillations in fixed-field alternating-gradient (FFAG) accelerators has been dis-

¹² Proposal for a High-Energy Accelerator (MURA, March 14, 1958).

¹³ O'Neill, Barber, Richter, and Panofsky, A Proposed Experiment on the Limits of Quantum Electrodynamics, Stanford University, May, 1958. Received and reprinted June, 1959.

¹⁰ E. D. Courant and H. S. Snyder, *Ann. Phys.* **3**, 1 (1958).

¹¹ R. Q. Twiss and N. H. Frank, *Rev. Sci. Instr.* **20**, 1 (1949).

cussed by Symon, Jones, Kerst, Laslett, and Terwilliger.⁹ There also betatron oscillations damp as $B^{-\frac{1}{2}}$.

The radial beam spread due to synchrotron oscillations damps in a manner which has been discussed by Symon and Sessler (reference 8) for the case of fixed-field synchrotrons. Calling θ the azimuthal angle, they find a corresponding generalized momentum $W = \int [dE/\omega]$, where ω is the particle rotation frequency. (W, θ) are shown to be a set of canonical variables; area in the (W, θ) space is therefore conserved. On translation to ordinary coordinate space, their result is identical to that of Twiss and Frank.¹⁴ The damping factors for betatron and synchrotron oscillations are therefore the same in all proton accelerators, whether weak or strong focusing, fixed or variable field. In electron accelerators the radiation produces strong damping effects; above a few hundred Mev these effects dominate the adiabatic damping.

The number of accelerated bunches which can be stacked within the available synchrotron oscillation phase space in a storage device of 3 to 25 Bev is at most a few thousand; much less if a high-current linear accelerator of the usual energy spread is used as the original low-energy injector. Even present-day high-energy accelerators, with repetition times of a few seconds, would therefore be able to fill the available phase space in a beam storage device in less than the calculated beam lifetime. In practice it would be quite difficult to make use of more than a small fraction of the total phase space; a numerical example is given in Sec. V.

In comparing further the various possible beam-stacking devices, we must note that the translation from phase space to ordinary coordinate space involves three quantities: the vertical and radial betatron wavelengths and the momentum compaction factor $\alpha = (\dot{p}/r) \times (dr/d\dot{p})$. As will be made clear by a numerical example, strong vertical focusing and a high value of α^{-1} are needed in a beam stacking system.

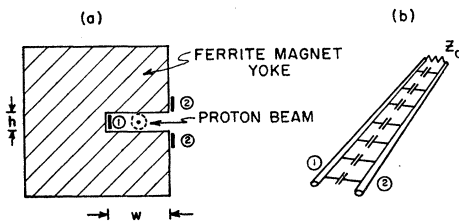


FIG. 2. (a) Delay-line deflector, for ejecting protons from a synchrotron and injecting them into a storage ring. 1 and 2 are the forward and return sections of the (one-turn) winding. (b) External capacitors connect 1 and 2 by leads across the magnet pole faces, to give the delay-line characteristic impedance Z_0 .

¹⁴ Due to a copying error in the derivation, Eqs. (19) and (21) of reference 8 differ from the corresponding equations of Twiss and Frank. The error does not, however, carry through to numerical estimates quoted by the MURA group.

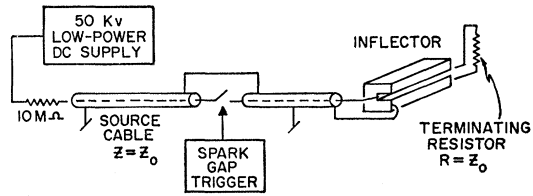


FIG. 3. Delay-line inflector circuit diagram. The bending angle given the protons is proportional to the voltage of the dc supply. The turn-on time of the magnet is the transmission time of the pulse through it, and the duration of the pulse is twice the delay time of the source cable.

The following sections will take up the special problems which must be solved if the acceleration and beam-storage guide fields are separate.

III. BEAM TRANSFER

(a) Method

In order to obtain efficient beam transfer, one should pulse on a uniform magnetic field of well-controlled focusing properties in a time which is small compared to one beam revolution period. This magnetic field should then be held constant for one turn. The deflected beam can then pass through a dc magnet capable of producing a large bending angle; identical units would be used to inject the transferred beam into the storage ring.

The delay-line inflector,¹⁵ which was designed for this purpose, consists of a ferrite-core magnet with a shaped air gap (see Fig. 2). It is convenient to consider the ferrite-core magnet as having a distributed inductance of L henries/m. If the magnet is loaded with a distributed capacitance of C farads/m, it becomes a delay line with characteristic impedance $Z_0 = (L/C)^{\frac{1}{2}}$.

The delay time is $\tau = l(LC)^{\frac{1}{2}}$, where l is the physical length of the magnet. This delay line is terminated in its characteristic impedance and driven by a charged coaxial cable through a spark gap (see Fig. 3). After the delay time τ the magnetic field throughout the line assumes a constant value. The duration of the magnetic field is twice the delay time of the source cable. In order to bend particles of momentum p (mks units) through an angle θ , the pulse voltage required to turn on the magnet in time τ is $V = (p\theta/e\tau)(w+h)$, where w and h are the width and height, respectively, of the magnetic gap. To minimize the required voltage V , τ is made as large as tolerable. It must be kept small compared to a particle circulation time. Possible values for the parameters at 25 Bev are $\tau = 0.25$ microseconds (in order to lose only 10% of the synchrotron beam on ejection) and $w+h = 4$ cm. A single magnet with a pulse voltage of 20 kv would produce a bending angle of 0.12 degrees. Three such magnets, operating in series on the beam but in parallel electrically, could displace the 25-Bev

¹⁵ G. K. O'Neill and V. Korenman, Princeton-Pennsylvania Accelerator Project, Internal Report, GKO'N-10 VK-3, November, 1957 (unpublished).

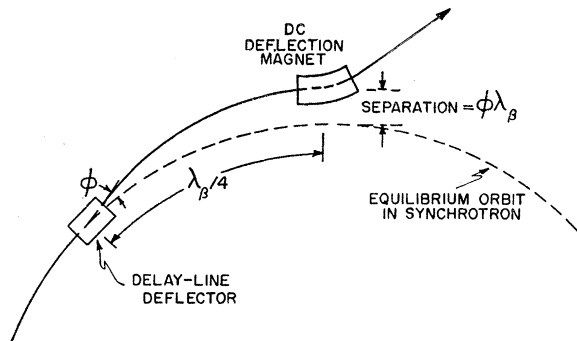


FIG. 4. Combination of pulsed and dc bending magnets for ejection of particle beam without loss of particle density. λ_β in figure should read λ_β .

beam by 9 cm into the gap of a dc magnet for further deflection (see Fig. 4). Although the delay-line inflector is limited to a peak field of about 3 kilogauss by ferrite saturation, the straight-section lengths required for the inflector are not excessive. At 25 Bev the 3-section magnet needed for a 9-cm beam deflection would be only 6 feet long, and would weigh about 200 pounds. Such a mass could easily be moved into position during the acceleration cycle of a large synchrotron. The high-voltage power supply to charge the coaxial cable for driving the inflector would need to deliver only 200 watts.

It is important to note that *no* betatron oscillations need be induced by such a process, and that the beam would emerge from the synchrotron within one revolution period with almost no loss of particle density.

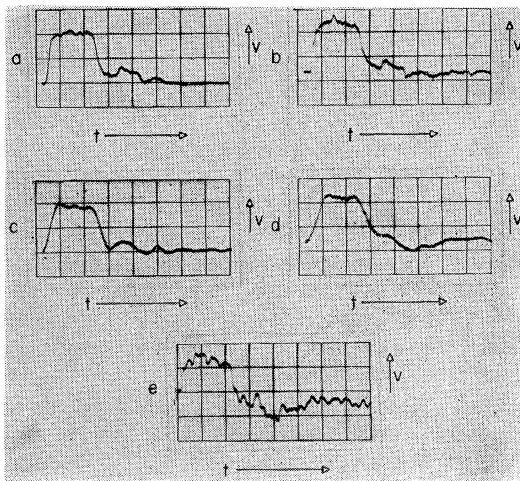


FIG. 5. Behavior of a delay-line inflector driven by a 10-ohm cable. 200-volt pulse with length of 100 millimicroseconds. (a) Cable discharged into a 10-ohm resistor. (b) Same, except delay-line inflector interposed between switch and resistor. (c) Same as (a) except 25-kv pulse, with spark switch substituted for mercury switch pulser. (d) Same as (c), except inflector inserted before terminating resistor. (e) Magnetic field in gap of inflector, observed by shielded loop with integrating circuit, through oscilloscope amplifier. Signals (a) through (d) are put directly on oscilloscope plates without amplification.

This is in contrast to existing methods of high-energy beam deflection, which lose most of the original particle density through scattering (as in the Brookhaven 3-Bev ejector), or through the excitation of large betatron oscillations (as in the regenerative extractor system).

Small errors in pulse height applied to the deflectors would cause no loss of density in synchrotron oscillation phase space, because these magnets would not affect particle energy. The small increase in radial betatron oscillation amplitudes caused by such errors would not, in most simple beam-stacking systems, affect the current density in ordinary coordinate space.

(b) Experimental Results on Inflector

A delay-line inflector magnet, 10 cm long with a 1-cm vertical aperture, has been built to operate at a characteristic impedance of 10 ohms. It is pulsed through a triggered three-element spark gap from a 10-ohm cable charged to 50 kv. The delay cable provides a pulse 100 millimicroseconds long, 25 kv high. With these parameters the magnetic field in the gap of the inflector reaches a peak of 3000 gauss. The delay time through the inflector is 50 millimicroseconds and its contribution to the rise time (due to the lumped-constant condensers used in place of true distributed capacity) is less than 20 millimicroseconds.

This inflector is one of three sections intended for use in an electron scattering experiment at 500 Mev. Although the inductance of the spark gap distorts the rectangular pulse which should be applied to the inflector, the observed pulse shape on the terminating resistor beyond the inflector is almost identical to that which is applied at the inflector input (see Fig. 5). The magnetic field within the gap, as measured by a shielded one-turn pickup coil and integrating network, follows the applied signal with little distortion. As expected, the behavior of the inflector as a circuit element is linear both for 200-volt and 25-kv pulses.

Although this model is already adequate for its intended purpose, some simple improvements in its spark-switch driver are being made. If used in a proton storage ring system, the pole faces of a delay-line inflector could if necessary be ground to produce a field of arbitrary uniformity at a designed operating point. The material cost and development time required to bring the inflector to its present stage are both small.

(c) Emittance Matching

As noted earlier, the synchrotron oscillation phase density is not affected by errors in the beam transfer system. It is, however, also important that no serious losses of betatron phase density occur during transfer, particularly in the vertical direction. In general, with different betatron wavelengths in accelerator and storage rings, density losses will occur unless a matching lens is included somewhere in the transfer path. The

final beam size in the synchrotron determines the size and angular spread of the ejected pulse. Consider a beam with a maximum vertical spread Δz whose particles have random directions up to a limiting angle $\Delta\theta$. It is convenient to define the "emittance" of the beam as¹⁰

$$\epsilon = \pi \Delta z \Delta \theta.$$

Simple magnetic lens systems can be designed which hold the emittance constant, but which alter the ratio of Δz to $\Delta\theta$. For example, a positive thin lens with a linear magnification M magnifies the angular divergence by M^{-1} . A quadrupole magnet pair is a good approximation to such a thin lens. In the synchrotron, the region in (z, θ) phase space occupied by the beam is roughly an ellipse, with semi-axes Δz and $\Delta\theta$. These are related by $\Delta z = \lambda_s \Delta\theta$, where $2\pi\lambda_s$ is the betatron wavelength in the synchrotron. If the beam is transferred without matching to a storage ring of different λ , each particle will still move on an elliptical path in phase space, but the particle group as a whole will have in addition a coherent betatron oscillation; the ellipse which encloses the particle group in phase space will itself rotate within a larger ellipse. A matching lens can prevent the coherent oscillation by adjusting the Δz and $\Delta\theta$ of the beam injected into the storage rings to satisfy $\Delta z = \lambda_R \Delta\theta$, where $2\pi\lambda_R$ is the betatron wavelength in the storage rings. In going from a weak-focusing synchrotron to a strong-focusing storage ring, the particle density can actually be increased by this process. The matching system should make the final circulating beam in the storage ring independent of the focusing properties of the injecting synchrotron. Regarded as an injector for storage rings, a useful figure of merit for an accelerator is therefore $Q/\epsilon^{1/2}\Delta E$, where Q is the accelerated charge per pulse, ΔE is the energy spread, and ϵ is the emittance of the accelerated beam.

(d) Injection

The particles to be stored would pass through the following sequence: acceleration in the synchrotron, delay-line deflector, dc ejector, steering magnets, matching lens, dc injector, and delay-line inflector (see Fig. 6). During the interval before the next acceleration cycle (0.05 to 5 seconds for large synchrotrons), the newly injected pulse could be moved by slowly shifting the frequency of a low-power rf cavity.⁸ In this manner it could be stacked next to previously stacked beam pulses at the far side of the vacuum chamber. If the delay-line inflector were placed at the inner limit of the storage ring's good- n region, the stacking process would produce a small amount of additional acceleration. In a small-aperture storage ring the additional energy obtained in this manner would be 3 to 5% (c.m. system).

IV. STORAGE RING DESIGN

Several geometries are possible for the storage rings in which the accelerated particles would be stacked.

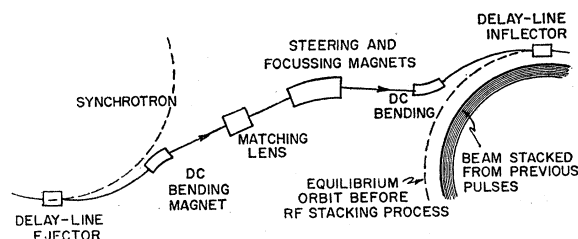


FIG. 6. Ejection-injection sequence. Except for the delay-line deflectors and the synchrotron itself, all magnets are constant-field. The low-power rf system in the storage ring needs only to produce a stable phase region large enough to contain a single synchrotron pulse, and it has available the full recycling time of the synchrotron in which to perform the stacking operation.

For maximum utility in carrying out experiments, it is desirable that several easily accessible interaction regions be available simultaneously. In these regions, the vacuum chamber should have a small cross section, and the nearest guide-field magnets should subtend the smallest possible solid angle. The magnets and magnet coils should be of simple design and construction. Finally, the over-all structure should be of minimum physical size and weight.

The two-way FFAg synchrotron design of Ohkawa⁴ satisfies the first requirement, having several experimental areas. An improved storage-ring geometry (suggested by a consideration of the advantages and limitations of the Ohkawa design) has been developed⁵ (see Fig. 7). In this concentric storage-ring design (hereafter called CSR), each beam particle would travel through the following sequence: a sector of radius R_1 , a straight section of length l , another sector of radius R_2 , and another straight section (also of length l). In the Ohkawa design it is necessary to use reversed field magnets in order that two beams may circulate in

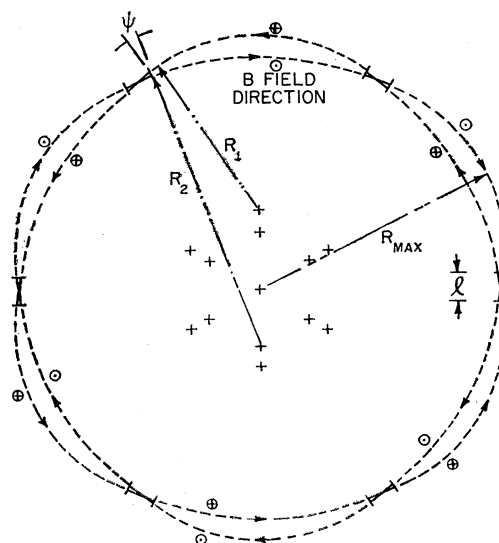


FIG. 7. Particle orbits in a concentric storage ring with six straight sections.

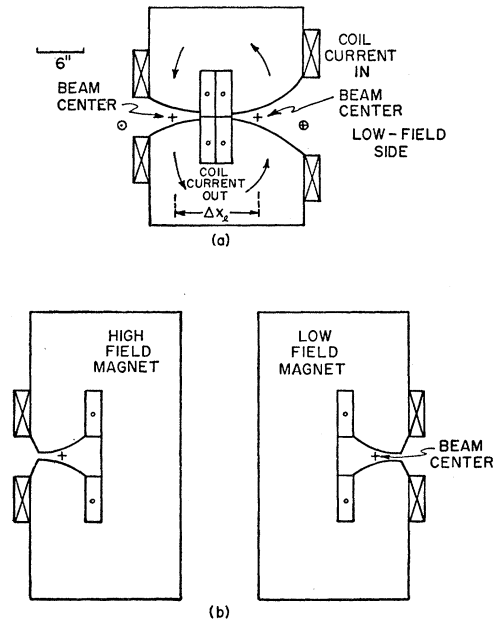


FIG. 8. Concentric storage ring magnet cross-sections. (a) At end of straight sections. (b) Near center of curved sectors.

opposite directions in a single guide field containing a wide momentum spread. Consequently the Ohkawa design has a large circumference factor (defined as the maximum ratio of machine radius to particle radius of curvature). In the CSR no reversed field magnets are used. The momentum spread contained in the CSR can be small, because acceleration takes place in the separate guide field of the injecting synchrotron. For these reasons the magnet weight in the CSR design is reduced from that of the Ohkawa synchrotron.

(a) CSR Parameters

The ideal design would have a large number of long straight sections and a small beam crossing angle. In the choice of design parameters, however, it should be noted that the separation between the circulating beams at the end of each straight section, Δx_i (see Fig. 8), must be large enough to permit placing magnet coils between the circulating beams at the magnet ends. For a given straight section length, this sets a minimum

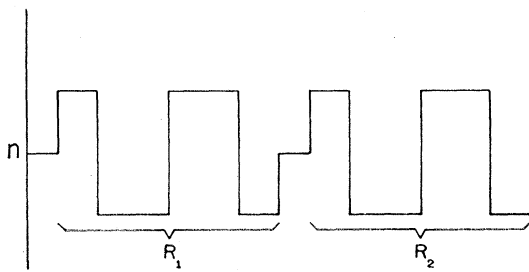


FIG. 9. Magnet cell structure for 3-Bev concentric storage ring. n is the field gradient index.

value on the beam crossing angle ψ , and hence on the circumference factor.

With the notation of Table I, an approximate formula for the circumference factor is

$$C.F. \cong 1 + \frac{\sin(\psi/2) + l/2R_1}{\sin(\theta/2)}.$$

The physical size of a CSR would exceed by about 25% that of a conventional synchrotron having the same number and length of straight sections, and limited to the same peak magnetic field. Parameters for three possible CSR designs are listed in Table II. $W_s + W_{CSR}$ is the total magnet weight including that of the injecting synchrotron. The published data on a two-way FFAG synchrotron design of equal energy¹² are also listed. T_E is the energy of a conventional stationary-target synchrotron yielding the same center-of-mass energy.

(b) Magnet Cell Structure

The magnet cell structure for a CSR could be either constant-gradient (CG) or alternating-gradient (AG). However, the stronger focusing in AG cell structures would permit much larger circulating currents for a given $Q/\epsilon^3 \Delta E$. Consequently only AG cell structures will be considered. In a CSR, the circumference factor is independent of the focusing properties.

Stability diagrams for the first CSR design in Table II have been calculated with an IBM 704 using standard matrix methods.¹⁰ The results presented here assume 24 magnets per ring. If the guide fields in each sector had the same radius of curvature the machine would be circular and have a symmetry of six. Because of the different radii of curvature the machine actually has a symmetry of three. Hence a unit cell (see Fig. 9) consists of eight magnets and two straight sections. For simplicity the two focusing magnets in the same sector have the same n value, and similarly for the two defocusing magnets. This still leaves four free parameters. However, by scaling the corresponding n values from one sector to the next, two of these free parameters are eliminated. The n values are chosen nearly proportional to the particle radii. Consequently the actual magnetic field gradients are very nearly the same in all focusing magnets, and similarly for the defocusing magnets. More precisely, the scaling factor is chosen so that for corresponding magnets in either sector, $(n/R)^{1/2}(s-s_0)$

TABLE I. Geometrical parameters for concentric storage rings.

N	= number of straight sections
$\theta = 2\pi/N$	
ψ	= beam crossing angle
l	= straight section length
R_1	= smaller particle radius
R_2	= larger particle radius
Δx_i	= separation between circulating beams at end of straight sections

TABLE II. Design parameters for several intersecting-beam systems.

Parameter	CSR	CSR	FFAG	CSR	Unit	Remarks
Energy	3	15	15	25	Bev	
T_B	30	540	540	1500	Bev	
R_{max}	16.8	74	183	114	meters	
B_{max}	11	11	18	11	kilogauss	a
Circumference factor	1.45	1.35	5.8	1.25		b
N	6	8	4	8		c
Straight section length	1.8	4.9	9.5	6.1	meters	d
Crossing angle	0.29	0.155	0.18	0.126	radians	
Δx_l	0.27	0.38		0.38	meters	e
Superperiods/revol.	3	4	2	4		
Radial betatron wavelength	26	70	40	116	meters	
Vertical betatron wavelength	24	64	226	107	meters	
W_{CSR}	600	4300		7000	tons	f
$W_s + W_{CSR}$	950	6700	65 500	11 000	tons	g
W (iron alone)	900	6200	62 500	10 000	tons	
W (copper alone)	50	500	3000	1000	tons	
Power	2	10	45	15	Mw	
Vacuum chamber	5×15	5×15	15×480	5×15	cm	h

^a Held to 11 kilogauss in CSR to permit varying energy without changing interaction region position.
^b Should be doubled if CSR located outside synchrotron.
^c Number of straight sections available for intersecting-beam experiments.
^d Interaction region located close to one end in FFAG case.
^e Orbit separation at ends of straight sections.
^f For 15-Bev CSR, magnet cross section same as BNL 25-Bev synchrotron.
^g Total weight of synchrotron plus CSR.
^h Vacuum chamber is double walled in FFAG case.

has the same value, where $(s-s_0)$ is the distance along the equilibrium orbit. It should be noted that, because of the different radii of curvature, the stability diagram is no longer completely symmetrical between the vertical and radial betatron oscillations.

Some of the above assumptions have been made principally for mathematical simplicity. Therefore, it is probable that this is not an optimum design. Figure 10 shows the stability diagram obtained. The n values on the graph are the geometric means of the n values in the sectors of different curvature. The splitting of the fundamental stability diagram along lines AA and BB

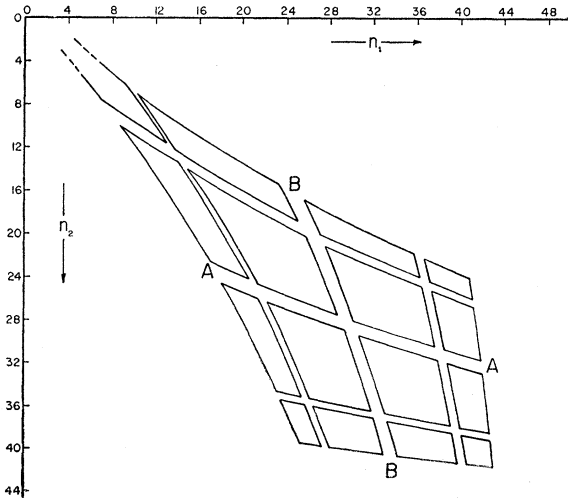


FIG. 10. Fundamental stability diagram for 3-Bev concentric storage ring. Stop bands AA and BB are due to straight sections. Other stop bands are due to alternating radii of curvature.

is due to the straight sections. The remaining stop bands are due to the alternating radii of curvature. It should be noted that the magnets next to the straight sections are shorter than the magnets in the middle of the sectors. The ratio of lengths was chosen so as to obtain a fairly good stability pattern, but has not been optimized.

Figure 11 is an expanded view of the high- n region of Figure 10. The principal resonances have been included, following the diagram given by Sturrock.¹⁶ The operating point indicated on Fig. 11 would be satisfactory.

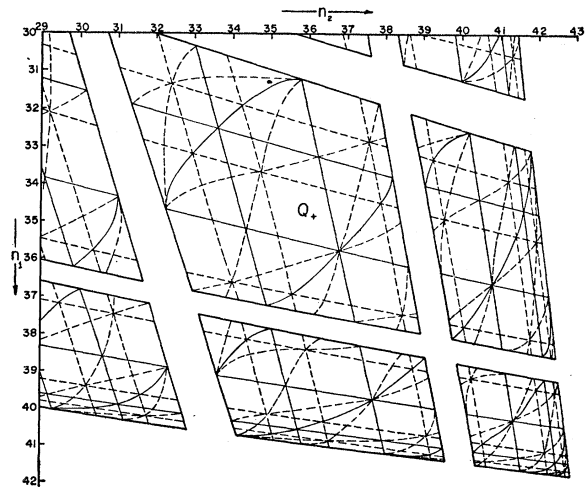


FIG. 11. High- n region of fundamental stability diagram for 3-Bev concentric storage ring. Principal resonances have been included. Q indicates possible operating point.

¹⁶ P. A. Sturrock, Ann. Phys. 3, 113 (1958).

(c) Layout

The layout of the synchrotron and CSR would be fairly flexible. At 3 Bev it would probably be simplest to use a single ejection point and several dc bending magnets. At 25 Bev the use of two ejection points would avoid many degrees of bending in the transfer system (see Fig. 12). It would also be possible to locate a CSR concentric with, and either inside or outside of, a large AG synchrotron, whose direction of acceleration could be reversed over a period of a few minutes with the help of a beam bending magnet for its own injector. If the synchrotron were originally intended to be used with a CSR, it would be possible to design the synchrotron without regard to experimental use, except for straight sections set aside for beam ejection. Since very little of the synchrotron beam should be lost during the transfer, all single-beam experiments could be performed in the CSR, where a unity duty cycle would be available without primary beam energy spread. The components of a CSR should be considerably more resistant to radiation than the organic seals, insulators and vacuum chamber of a rapid-cycling synchrotron. There should be maintenance advantages in transferring the radioactivity produced in a high-intensity accelerator to the simple dc magnets, low-voltage coils, and all-metal vacuum chamber of a CSR.

V. INTERACTION RATE

In order to calculate the beam-on-beam interaction rate only the following parameters are necessary:

- z = vertical beam height in CSR,
- I = circulating current in CSR,
- ψ = beam crossing angle.

For a process with cross section σ , the interaction rate Y is then given approximately by

$$Y \cong \frac{2(I/e)^2 \sigma}{cz \sin \psi},$$

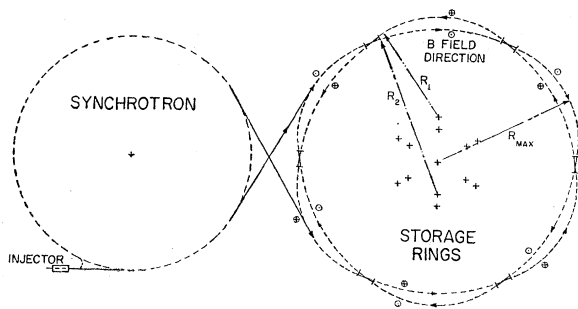


FIG. 12. One of several possible arrangements of a high-energy synchrotron and concentric storage ring to minimize required number of steering magnets. The synchrotron would be equipped with a magnet to reverse the low-energy beam of its injector. The direction of acceleration would be reversed at intervals of a few minutes.

where e is the proton charge and c is the velocity of light. The interaction rate is independent of the radial spread of the beams. To calculate z , the vertical amplitude functions¹⁰ $\beta(s)$ for both the synchrotron and CSR must be known, as well as the vertical beam height z' in the synchrotron. Ideally, the vertical height in the CSR would then be $z = z'(\beta_{\text{csr}}/\beta_{\text{sync}})^{1/2}$. Allowances for losses during the beam transfer must be made. The detailed variation of the amplitude function is taken into account by the form factor $F = \beta_{\text{max}}/\beta_{\text{Av}}$. As an example, in the case of the Princeton-Pennsylvania 3-Bev proton synchrotron, we assume that initially the vertical betatron oscillations fill the two inches of vertical aperture. Since these oscillations damp as $B^{-1/2}$, the vertical beam spread on ejection may be found. In the synchrotron B goes from 270 gauss to 13.8 kilogauss, and $\beta_{\text{Av}} = 43.4$ (with $F \approx 1$). The present CSR design gives $\beta_{\text{Av}} = 12.3$ (with $F \approx 3$). Assuming a 50% loss in vertical betatron density during transfer, we finally obtain $z_{\text{Av}} = 0.7$ cm in the CSR. In this design the value of z in the interaction region is approximately z_{Av} .

To calculate I , it is necessary to know the momentum compaction α ,¹⁰ and the shapes of the equilibrium orbits for the CSR and synchrotron, as well as the radial spread of the beam due to synchrotron oscillations. Ideally, the number of beam pulses that could be stored in the CSR is then given by $(\Delta r_r/\Delta r_s)(\alpha_s/\alpha_r)$, where Δr_r is the width of the CSR's good- n region, and Δr_s is the radial width occupied by phase oscillations at ejection time in the synchrotron. The corrections for the shapes of the equilibrium orbits may be obtained, to first order, from the form factor F for the radial amplitude function. In the case of the Princeton-Pennsylvania synchrotron, we assume that initially the radial synchrotron oscillations fill the six inches of good- n region. Noting that these oscillations damp as B^{-1} , the radial spread due to energy oscillations at ejection may be calculated. There should be roughly 4 inches of good- n region in the CSR. In the synchrotron $\alpha = 2.1$, and in the CSR $\alpha = 0.07$. We assume 3×10^{10} protons/pulse in the synchrotron (about $\frac{1}{6}$ of the design current). Assuming a 50% loss of particles during transfer we obtain $I/e \approx 2 \times 10^{19}$ sec.

However, it should be noted that in the synchrotron, the protons will not be uniformly distributed in phase at ejection. Rather, they will be bunched about the stable phase point. For the Princeton-Pennsylvania synchrotron the phase spread on injection will be ~ 180 degrees. If the rf voltage can be turned off adiabatically, the beam pulse will spread uniformly around the machine. Because the area in synchrotron phase space will be conserved during this process, the beam will shrink radially. In a rapid-cycling synchrotron there is, however, reason to doubt that the rf can be turned off adiabatically. There remains the interesting possibility of making the storage ring circumference a multiple of the final separation between stable phase points in the injecting synchrotron, so that adiabatic turn-off can be

carried out at leisure by the low-power stacking rf system of the storage ring. We have assumed non-adiabatic turn-off in order to reach a conservative estimate of the final interaction rate.

The 3-Bev CSR design of Table II gives a circulating current of 3.2 amperes at 2 amp/cm². The proton-proton reaction cross section at 3 Bev is approximately 30 mb. Formula (1) then gives 4000 reactions per second. (A factor of ~ 1000 has been thrown away in various safety factors.) Assuming a vacuum of 10^{-9} mm in the CSR,¹⁷ the interaction rate due to the residual gas in one straight section would be roughly five times larger than the total beam-on-beam interaction rate, with the safety factors assumed. In arriving at the interaction rate quoted here, we have gone into the details of a particular acceleration system. No use has been made of vertical oscillation phase space, because as a practical matter it is somewhat difficult to fill. It also happens that in any acceleration system, with fixed or variable field, it is very difficult to make use of the narrow energy spread obtainable from an electrostatic injector. A van de Graaff generator can fill a narrow region only one or two kv wide in synchrotron phase space. When the rf voltage comes on, however, each injected particle will begin to move on an elliptical path in phase space; particles near the limits of stable phase will oscillate over an energy range $\Delta E = [8VE/\pi h|\kappa|]^{\frac{1}{2}}$, where V is the rf voltage, h is the harmonic order, E is the whole energy, and $\kappa = (E/\omega) \times (d\omega/dE)$ is at van de Graaff energies a number of magnitude 100 to 300 for all synchrotrons, strong or weak focusing, fixed or variable field. At the low value of $V=1$ kv, ΔE is about 120 kv for $h=1$. Even at very low rf voltages and high harmonic orders there is a mismatch of about a factor 10 between the van de Graaff's energy spread and the separatrix size in the synchrotron. In the example used above, it is assumed that the injector is intentionally modulated over 40 kv during the injection time; this increases the accelerated charge per pulse and is in fact the way the Princeton-Pennsylvania synchrotron has already been designed to operate. In our example, the available synchrotron phase space in the CSR can be filled by about 300 pulses from the accelerator.

We have also assumed no manipulation of the radial betatron phase space. In principle, the final current density could be increased by allowing the radial betatron amplitude to equal the radial beam size set by energy spread. If the accelerator and the beam transfer system can be made to work to their design limits, and if use is made of vertical (but not radial) betatron phase space, the interaction rate density can be increased above our estimates by a factor of about 500. The rate would then equal that of 3×10^9 protons/5 sec on a liquid hydrogen target.

¹⁷ D. Grove, Project Matterhorn, Princeton University, Technical Memo No. 40 (unpublished).

VI. ACCELERATION IN THE CSR

After the available phase space in a CSR was filled by beam pulses from the injecting accelerator, the CSR magnetic field could in principle be increased, so that the stored beam could be further accelerated.¹⁸ A very slow increase of the field, to avoid eddy-current field perturbations in the solid-iron magnets, could still be performed within a small fraction of the calculated beam lifetime. The required rf power for the acceleration system would be a very steep function of the energy spread to be accommodated (unless phase displacement acceleration⁸ were used). For a 2% relative energy spread at 3 Bev, the instantaneous peak rf power during acceleration could, however, be held to less than 50 kw. Only one or two percent of frequency shift would be required. For the 3-Bev synchrotron used before as an example, a CSR of 30 meters radius and magnet weight of 1200 tons could give a center-of-mass energy of 6 Bev/proton, with $T_E=100$ Bev.

VII. DESIGN OF EXPERIMENTS

The interaction regions of a CSR would be at the centers of the long straight sections. The locations of the interaction regions would not depend on beam energy. In a 15-Bev CSR, the nearest magnets would subtend a solid angle of about 0.15 steradian at each interaction region. It is expected that reaction products will be confined to forward and backward cones in the center-of-mass system. If no attempt were made to increase interaction rates by filling vertical betatron phase space, the circulating beams would be about 0.5 cm high. Detection apparatus could be placed within 3 cm of the interaction region in the vertical direction, and within 10 cm radially.

At present the large volume of the interaction region would limit experiments with proton intersecting-beam devices to the use of bubble chambers or the scintillation cameras now under development. However, it has been pointed out by Courant that in the simple linear magnet cell structure of a CSR, it should be possible to insert quadrupole magnets. These could cause the equilibrium orbits to cross at the center of each straight section. Although the total interaction rate would be no higher, the source brilliance would then be high enough so that counter work with secondary beam analysis would become practical. (*Note added in proof.*—Orbits for a CSR modified as above have been calculated, and shown to cross as predicted.)

It has usually been assumed that magnetic analysis of the interaction region would be impossible in a colliding beam device. However, in principle there is no reason why a magnetic field could not be added to an interaction region, if balanced by oppositely directed fields at the ends of the same straight section. It might be necessary to put in identical magnets at every

¹⁸ E. J. Woods, Princeton-Pennsylvania Accelerator Project, Internal Report EJV-1, August, 1958 (unpublished).

straight section, in order to preserve the symmetry of the CSR.

At present the last two suggestions are speculative, but they can be checked by standard matrix methods. One should note that the simplicity of the CSR magnet cell structure permits a great economy in computations. All of the work reported here, including the stability diagrams, required about 2 hours of 704 computer time.

VIII. CONCLUSIONS

Any accelerator working between given initial and final energies appears to be subject to the same limitations on final circulating current density as measured in the appropriate phase space. It also seems that even a slow-cycling (one pulse/5 seconds) synchrotron could fill the phase space available in a beam storage device within a small fraction of the calculated lifetime of a stored beam. For these reasons it has seemed to us well worthwhile to look into the difficulty (previously assumed very large) of transferring the full beam of a synchrotron to a storage ring without serious density losses. From our measurements on the simple inflector described in Sec. III, we conclude that transfer with high efficiency should be quite easy.

The over-all design of an intersecting-beam system appears to be much simplified if one can attack the acceleration and beam storage problems separately; this simplification is accompanied by a reduction of about a factor ten in the weight of the system, and a somewhat smaller reduction in over-all size. The storage-ring arrangement seems to offer several advantages for experimental use, mainly due to its small vacuum chamber and magnet cross section.

IX. SUGGESTIONS FOR FURTHER WORK

The orbit dynamics of a CSR are given by linear alternating-gradient theory,¹⁰ which has been well checked by the successful operation of the Brookhaven

1-Mev electron model and the Cornell 1-Bev electron synchrotron. The interaction region forces could, however, be checked by building a small electron model of the CSR. Operation at 10 Mev with a one-meter diameter and a field of 800 gauss would permit the use of a commercially available linac for testing.

It would be a modest undertaking to perform two tests which might be of greater value. One would be to build, full scale, a beam transfer system for an existing large proton synchrotron. After leaving the delay-line ejector, the transferred beam could travel down a long field-free vacuum pipe, where its stability and emittance could be studied by counters and by remote-viewing of scintillator plates.

A second worth-while test would be the construction of a vacuum chamber for a CSR, full scale in cross section but only several tens of feet long. If this model were combined with an inflector system, the effect of high-energy radiation on the operation of an ultrahigh vacuum system could also be studied.

ACKNOWLEDGMENTS

We wish to acknowledge helpful discussions with D. Judd, Lloyd Smith, E. Courant, H. Snyder, F. C. Shoemaker, C. J. Tsao, and M. G. White. It is a pleasure to thank the many members of the MURA group for their constructive criticism, and for several illuminating comments on orbit theory. The whole concept of phase space manipulation is due largely to the MURA theoretical group, and our use of rf beam stacking techniques is taken directly from their work. One of us (G. K. O'Neill) wishes particularly to thank K. Symon, F. Cole, K. Terwilliger, F. Mills, and M. Keith for an informative trip to MURA, and A. Sessler, L. J. Laslett, and L. Jones for useful discussions on other occasions.

The construction and testing of the delay-line inflector was done by V. Korenman; support for this work from the Higgins Scientific Research Fund is gratefully acknowledged.

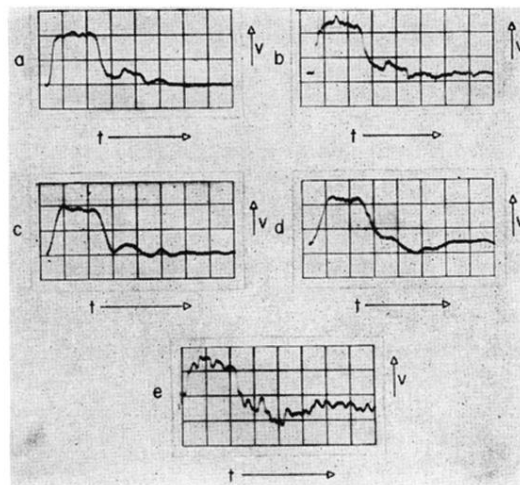


FIG. 5. Behavior of a delay-line inflector driven by a 10-ohm cable. 200-volt pulse with length of 100 millimicroseconds. (a) Cable discharged into a 10-ohm resistor. (b) Same, except delay-line inflector interposed between switch and resistor. (c) Same as (a) except 25-kv pulse, with spark switch substituted for mercury switch pulser. (d) Same as (c), except inflector inserted before terminating resistor. (e) Magnetic field in gap of inflector, observed by shielded loop with integrating circuit, through oscilloscope amplifier. Signals (a) through (d) are put directly on oscilloscope plates without amplification.